Published in final edited form as:
Mol Cancer Res. 2013 July ; 11(7): 793–807. doi:10.1158/1541-7786.MCR-12-0600.

Bioactive lipids sphingosine-1-phosphate and ceramide-1-phosphate are pro-metastatic factors in human rhabdomyosarcomas cell lines, and their tissue level increases in response to radio/chemotherapy

Gabriela Schneider[1], **Ewa Bryndza**[1], **Ahmed Abdel-Latif**[2], **Janina Ratajczak**[1], **Magdalena Maj**[1], **Maciej Tarnowski**[3], **Yurij Klyachkin**[2], **Peter Houghton**[4], **Andrew J. Morris**[2], **Axel Vater**[5], **Sven Klussmann**[5], **Magdalena Kucia**[1], and **Mariusz Z. Ratajczak**[1,2]

[1]Stem Cell Institute at James Graham Brown Cancer Center, University of Louisville, Louisville, KY [2]Division of Cardiovascular Medicine, Gill Heart Institute, University of Kentucky, Lexington, Kentucky, USA [3]Department of Physiology Pomeranian Medical University, Szczecin, Poland [4]World Children's Cancer Center, Columbus, OH [5]NOXXON Pharma AG, Max-Dohrn-Strasse 8-10, 10589 Berlin, Germany

Abstract

We observed that sphingosine-1-phosphate (S1P) and ceramide-1-phosphate (C1P) strongly enhance in vitro motility and adhesion of human rhabdomyosarcoma (RMS) cells. This effect was observed at physiological concentrations of both bioactive lipids, which are present in biological fluids, and is much stronger than the effects observed in response to known RMS pro-metastatic factors such as stromal derived factors-1 (SDF-1) or hepatocyte growth factor/scatter factor (HGF/SF). We also present novel evidence that the levels of S1P and C1P increase in several organs after γ-irradiation or chemotherapy, which indicates induction of an unwanted pro-metastatic environment related to treatment. Most importantly, we found that the metastasis of RMS cells in response to S1P can be effectively inhibited in vivo with the S1P-specific binder NOX-S93 that is based on a high affinity Spiegelmer. We propose that bioactive lipids play a previously underappreciated role in dissemination of RMS and the unwanted side effects of radio/chemotherapy by creating a pro-metastatic microenvironment. Therefore, an anti-metastatic treatment with specific S1P-binding scavenger such as NOX-S93 could become a part of standard radio/chemotherapy.

Keywords

sphingosine-1-phosphate (S1P); ceramide-1-phosphate (C1P); rhabdomyosarcomas; methastasis

Introduction

Rhabdomyosarcoma (RMS) is the most common soft-tissue sarcoma of adolescence and childhood and accounts for 5% of all malignant tumors in patients under 15 years of age (1,

Correspondence: Prof. Mariusz Z. Ratajczak MD, PhD, Hoenig Endowed Chair, Professor and Director Stem Cell Institute at James Graham Brown Cancer Center, University of Louisville, 500 S. Floyd Street, Rm. 107, Louisville, KY 40202, USA, Tel: (502) 852-1788, Fax: (502) 852-3032, mzrata01@louisville.edu.

Conflict of Interest: Gabriela Schneider and Mariusz Ratajczak received minor commercial research funding from NOXXON Pharma AG for studying the effect of NOX-S93 in chemo-radiation induced metastasis of RMS.

2). There are two major histological subtypes of rhabdomyosarcoma, alveolar rhabdomyosarcoma (ARMS) and embryonal rhabdomyosarcoma (ERMS). ARMS is more aggressive and has a significantly worse outcome than ERMS. Moreover, ARMS is characterized by the t(2;13)(q35;q14) translocation in 70% of cases or the variant t(1;13)(p36;q14) in a smaller percentage of cases (3). These translocations disrupt the *PAX3* and *PAX7* genes on chromosome 2 or 1, respectively, and the *FKHR* gene on chromosome 13, generating *PAX3-FKHR* and *PAX7-FKHR* fusion genes. These fusion genes encode the fusion proteins PAX3-FKHR and PAX7-FKHR which have enhanced transcriptional activity compared with wild type PAX3 and PAX7, and are postulated to play a role in cell survival and dysregulation of the cell cycle in ARMS (1).

It is well known that RMS cells, particularly in ARMS, are highly metastatic, belonging to the family of so-called “small round blue tumor cells”, which often infiltrate bone marrow (BM) and, because they can resemble hematological blasts, may sometimes be misdiagnosed as acute leukemia cells (2). A significant effort has been made to find chemoattractants that lead to metastasis of RMS cells to BM, and we and others have shown that the α-chemokine stromal-derived fctor-1 (SDF-1) and hepatocyte grow factor/scatter factor (HGF/SF) are secreted by bone marrow stroma and play an important role in RMS cell metastatic behavior (4, 5). The robust chemotactic response to these factors is also observed in in vitro migration assays in which both factors are employed as chemoattractants at supra-physiological concentrations (4, 5).

Since the concentrations of SDF-1 and HGF/SF in biological fluids and tissues is usually very low (6, 7), we began a search for other chemoattractants that could induce metastasis of RMS cells and turned our attention to bioactive lipids, such as sphingosine-1-phosphate (S1P) and ceramide-1-phosphate (C1P), as potential candidates. Both bioactive lipids have been reported to play an important role in development of skeletal muscle (8, 9), and, in addition, S1P has been demonstrated to direct migration of various types of tumor cells (10–12). It is known that S1P is secreted from several types of cells and binds to serum albumin and lipoproteins, all of which explains its relatively high (micromolar) concentration in peripheral blood and lymph (13). Similarly, the concentration of C1P is also comparably high in peripheral blood, and this bioactive lipid, which is retained intracellularly, may also be released from “leaky” cells following damage (13, 14). While five signaling receptors for S1P ($S1PR_{1–5}$) have been cloned and characterized, not a single receptor for C1P has been identified yet (15, 16). As reported already exposure of cells to S1P and C1P results in activation of signal transduction pathways involving MAPKp42/44 and AKT (16, 17).

One of the challenging problems of current radio/chemotherapy is recurrence and metastasis of cancer cells that survive initial treatment. We have proposed that one of the unwanted effects of radio/chemotherapy is induction of a pro-metastatic microenvironment in normal tissues damaged by treatment (18, 19), which suggests that standard anti-tumor treatment should be augmented by anti-metastatic therapy. Therefore, we were looking for a possibility to interfere pharmacologically with pro-metastatic factors such as S1P. To this end a promising candidate is NOX-S93, a mirror-image oligonucleotide that binds with high affinity and selectivity to S1P thereby inhibiting its activity (unpublished data). NOX-S93 is an inhibitor belonging to the class of so-called Spiegelmers (Spiegel = German word for mirror). These are biostable oligonucleotides made from non-natural mirror-image building blocks (L-nucleotides) that adopt complex three-dimensional structures and bind targets in a manner comparable to antibodies (20). Currently, three Spiegelmer-based compounds are in clinical development (21).

In this paper, we present novel evidence that S1P and C1P enhance motility and adhesive properties of RMS cells, and, since the levels of both bioactive lipids increase in several

organs after γ-irradiation or chemotherapy, induce an unwanted pro-metastatic environment after treatment. Most importantly, we found that the metastasis of RMS cells in response to S1P can be effectively inhibited in vivo by administration of this novel Spiegelmer NOX-S93 that binds and neutralizes S1P present in biological fluids. Based on this finding, we propose that anti-metastatic treatment with this anti-S1P compound could follow standard radio/chemotherapy.

Material and Methods

Cell lines

We used several human rhabdomyosarcoma cell lines (gifts from Dr. Peter Houghton, World Children's Cancer Center, Columbus, OH and Prof. Fred Barr, University of Pennsylvania, Philadelphia, PA), including both ARMS (RH4, RH5, RH18, RH28, RH30, RH41, CW9019) and ERMS (JR, SMS-CTR, RD, RH36) cell lines. SMS-CTR and RH36 cells were cultured in Dulbecco's Modified Eagle's Medium (DMEM) containing 10% fetal bovine serum (FBS), 100 U/ml penicillin, and 10 μg/ml streptomycin. All other cell lines were maintained in Roswell Park Memorial Institute (RPMI) medium 1640, containing 10% FBS, 100 U/ml penicillin, and 10 μg/ml streptomycin. Stromal cells were maintained in DMEM containing 20% fetal bovine serum (FBS), 100 U/ml penicillin, and 10 μg/ml streptomycin. All cells were cultured in a humidified atmosphere of 5% CO_2 at 37°C, and the media were changed every 48 hours.

Murine bone marrow stroma cells

Bone marrow derived stromal cells (MSCs) were expaned ex vivo from murine bone marrow mononucler cells (BMMNC) as described (17). Briefly, BMMNC were expanded in DMEM supplemented with 20% FBS and 50 U/ml penicillin/streptomycin for 7–10 days at 37°C in a 5% CO_2 incubator.

Real-time quantitative reverse-transcription PCR

Total RNA was isolated from RMS cells with the RNeasy kit (Qiagen, Valencia, CA). Human muscle RNA was obtained from Ambion (Austin, TX). The RNA was reverse transcribed with MultiScribe reverse transcriptase and oligo(dT) primers (Applied Biosystems, Foster City, CA). Quantitative assessment of mRNA levels was done by real-time reverse transcription PCR on an ABI 7500 instrument with Power SYBR Green PCR Master Mix reagent. Real-time conditions were as follows: 95°C (15 seconds), 40 cycles at 95°C (15 seconds), and 60°C (1 minute). According to melting point analysis, only one PCR product was amplified under these conditions. The relative quantity of a target, normalized to the endogenous β2-microglobulin gene as control and relative to a calibrator, is expressed as $2^{-\Delta\Delta Ct}$ (fold difference), where Ct is the threshold cycle, ΔCt = (Ct of target genes) − (Ct of endogenous control gene, β2-microglobulin), and ΔΔCt = (ΔCt of samples for target gene) − v(ΔCt of calibrator for the target gene). The following primer pairs were used: S1PR1-F, 5′-GCA TTA AAC TGA CCT CGG TGG T-3′; S1PR1-R, 5′-GGT CGG TGG AAT TTC TTG GTT-3′; S1PR2-F, 5′-CCC GAA ACA GCA AGT TCC A-3′; S1PR2-R, 5′-GAG AGC AAG GTA TTG GCT ACG A-3′; S1PR3-F, 5′-TTG CTG AAT GAA GCC GGA AC-3′; S1PR3-R, 5′-TCA CTT GGC ATT CAC AGA CGA-3′; S1PR4-F, 5′-CCG TCG AGG CTC ACT CCG GA-3′; S1PR4-R, 5′-GGG GCT CCC GCA TCC GAA AG-3′; S1PR5-F, 5′-CCC TCG TGG AAT TGA CGT TCT-3′; S1PR5-R, 5′-CCT GAC CAC CATC ACC ATC TCT-3′; β2-Microglobulin-F, 5′-AAT GCG GCA TCT TCA AAC CT-3′; and β2-Microglobulin-R, 5′-TGA CTT TGT CAC AGC CCA AGA TA-3′.

Cell proliferation

Cells were plated in culture flasks at an initial density of 1.25×10^4 cells/cm^2 in the presence or absence of S1P (1 μM) or C1P (0.5 μM). The cell number was calculated at 24, 48, and 72 h after culture initiation. At the indicated time points, cells were harvested from the culture plates by trypsinization and scored using FACS analysis.

Chemotaxis assay

Chemotaxis assays were performed in a modified Boyden's chamber with 8-μm pore polycarbonate membrane inserts (Costar Transwell; Corning Costar, Lowell, MA, USA) as described previously (22). In brief, cells detached with 0.05% trypsin were seeded into the upper chamber of an insert at the density of 3.5×10^4 in 110 μl. The lower chamber was filled with pre-warmed culture medium containing test reagents. Medium supplemented with 0.5% BSA was used as a negative control. In some experiments, cells were pretreated with 1 μg/ml pertussis toxin (PTX; Sigma-Aldrich, St. Louis, MO,) and the inhibitors U0126 (1 μM; Promega, Madison, WI), LY294002 (10 μM, Sigma-Aldrich), MK2206 (1 μM; Selleckchem, Houston, Tx), W146 (1 μM; Cayman Chemicals, Ann Arbor, MI), W140 (1 μM; Cayman Chemicals), JTE013 (1 μM; Cayman Chemicals), or BML241 (10 μM, Cayman Chemicals) for 15 min at 37°C. Inhibitors were also added to the lower chambers and were present throughout the duration of the experiment. After 24 hours, the inserts were removed from the Transwell supports. The cells that had not migrated were scraped off with cotton wool from the upper membrane and the cells that had transmigrated to the lower side of the membrane were fixed and stained with HEMA 3 (Protocol, Fisher Scientific, Pittsburgh, PA) and counted on the lower side of the membrane using an inverted microscope.

Phosphorylation of intracellular pathway proteins

RMS cell lines were kept overnight in RPMI medium containing low levels of bovine serum albumin (BSA, 0.5%) to render the cells quiescent. After the cells were stimulated with S1P (0.1, 0.5, or 1 μM) or C1P (0.5 or 1 μM) for 5 min at 37°C, they were lysed for 10 min on ice in RIPA lysis buffer containing protease and phosphatase inhibitors (Santa Cruz Biotech, Santa Cruz, CA). The extracted proteins were separated on a 12% SDS-PAGE gel and transferred to a PVDF membrane. The phosphorylation of serine/threonine kinase AKT (p-AKT473) and 44/42 mitogen-activated kinase (MAPK) was detected by phosphospecific mouse p44/42 and rabbit phosphospecific polyclonal antibodies (Cell Signaling, Danvers, MA, USA) with HRP-conjugated goat anti-mouse and anti-rabbit secondary antibodies (Santa Cruz Biotech). Equal loading in the lanes was evaluated by stripping the blots and reprobing with monoclonal p42/44 anti-MAPK antibody (clone no. 9102, Cell Signaling) and polyclonal anti-AKT antibody (Cell Signaling). The membranes were developed with an enhanced chemiluminescence (ECL) reagent (Amersham Life Sciences, Arlington Heights, IL), dried, and subsequently exposed to film (Hyperfilm, Amersham Life Sciences). The effect of different inhibitors on phosphorylation of AKT and MAPK kinases has been checked in experimental setting in which UO126, LY294002, MK2206 and PTx were added to the medium 2h before cell stimulation at concentrations employed in our chemotaxis experiments.

Adhesion assay to fibronectin

Cells were made quiescent for 3 hours with 0.5% BSA in RPMI 1640 before incubation with S1P (1 μM) or C1P (0.5 μM) for 1 hour. Subsequently, cell suspensions (5×10^3/100 μL) were added directly to 96-well plates covered with fibronectin and incubated for 10 min at 37°C. The wells were coated with fibronectin (10 μg/ml) overnight at 4°C and blocked with 0.5% BSA for 2 hours before the experiment. Following incubation, the plates were

vigorously washed three times to remove non-adherent cells, and the number of adherent cells was counted using an inverted microscope.

Adhesion assay to bone marrow-derived stroma cells

RMS cells were labeled before assay with the fluorescent dye calcein-AM and were made quiescent by incubation for 3 h at 37°C in RPMI 1640 medium supplemented with 0.5% BSA. The cells were then stimulated with S1P (1 μM) or C1P (0.5 μM) for 1 h at 37°C, then added to plates covered by mouse stromal cells, and incubated for 15 min at 37°C. After the non-adherent cells had been discarded, cells that adhered to the stromal cells were counted under a fluorescent microscope as described (4).

Fluorescent staining of RMS cells

RMS cells were fixed in 3.5% paraformaldehyde for 20 min, permeabilized by 0.1% Triton X100, washed in PBS, pre-blocked with 2% BSA, and subsequently stained with paxillin (1:200, mouse monoclonal IgG, eBioscience) and phalloidin-Alexa Fluor 488 (1:400, Molecular Probes, Eugene, Oregon). Appropriate secondary Alexa Fluor 594 goat anti-mouse IgG antibodies were used (1:400, Molecular Probes, Eugene, Oregon). The nuclei were identified by staining with DAPI (Molecular Probes, Eugene, Oregon). The fluorescence images were collected with a confocal microscope (Olympus, Center Valley, PA).

Knockdown of S1PR1 with short hairpin (sh)RNA

In RNAi experiments, the shRNA-generating plasmid pSUPER.retro.puro (Oligoengine, Seattle, WA) was used. The targeting base sequence for human S1PR1 was: 5′-AAG CAC TAT ATC CTC TTC TGC-3′. As a control, shRNA against Renilla was used with the targeting base sequence 5′-AAC AAA GGA AAC GGA TGA TAA-3′ (23). RMS cells were plated at 80% confluency and transfected with shRNA vector using Lipofectamine (Invitrogen, Carlsbad, CA) according to the manufacturer's protocol. RMS cells were plated at 80% confluency and transfected with shRNA vector using Lipofectamine 2000 (Invitrogen, Carlsbad, CA) according to the manufacturer's protocol. Selection of pSuper.retro.puro expressing cells was performed by exposure in in vitro cultures to puromycin at a final concentration of 5μg/ml for 3 weeks.

Preparation of conditioned media

Pathogen-free C57BL6 mice were purchased from the National Cancer Institute (Frederick, MD, USA), allowed to adapt for at least 2 weeks, and used for experiments at age 7–8 weeks. Animal studies were approved by the Animal Care and Use Committee of the University of Louisville (Louisville, KY, USA). Mice (four per group) were irradiated with 250, 500, 1000, or 1500 cGy. Twenty-four hours later, bone marrow, liver, lungs, and plasma were isolated. Conditioned media (CM) obtained by 1-h incubation of BM, liver, or lung cells (mechanically homogenized 30 times using a syringe) in RPMI at 37°C. After centrifuging, the supernatant was used for further experiments. In studies with the chemotherapeutic agent vincristine, mice were injected intraperitoneally with 0.9% NaCl with (0.5 mg/kg or 2 mg/kg) or without vincristine. Twenty-four hours later, organs were isolated and CM from various organs was prepared as described above.

Transplants of RMS cells into immunodeficient mice

To evaluate the in vivo metastatic behavior of two populations of RH30 cell lines (RH30 transfected with shRenilla and RH30 with knockdown of S1PR1), cells were injected intravenously (i.v.; 3×10^6 per mouse) into severe combined immunodeficient (SCID)-Beige inbred mice (five mice per group) that were either i) untreated (control), ii) irradiated

with 750 cGy 24h earlier or iii) exposed to 4-deoxypyridoxine (DOP) in drinking water as described previously (6). Marrows, livers, and lungs were removed 48 hr after injection of these cells, and the presence of RMS cells (i.e., murine-human chimerism) was evaluated as the difference in the level of human α-satellite DNA expression. DNA was amplified in the extracts isolated from BM-, liver-, and lung-derived cells using real-time PCR. Briefly, DNA was isolated using the QIAamp DNA Mini kit (Qiagen). Detection of human satellite and murine β-actin DNA levels was conducted using real-time PCR and an ABI Prism 7500 Sequence Detection System. A 25-μl reaction mixture containing 12.5 μl SYBR Green PCR Master Mix, 300 ng DNA template, 5′-ACC ACT CTG TGT CCT TCG TTC G-3′ forward and 5′-ACT GCG CTC TCA AAA GGA GTG T-3′ reverse primers for the α-satellite, and 5′-TTC AAT TCC AAC ACT GTC CTG TCT -3′ forward and 5′-CTG TGG AGT GAC TAA ATG GAA ACC-3′ reverse primers for the β-actin were used. The Ct value was determined as before. The number of human cells present in the murine organs (the degree of chimerism) was calculated from the standard curve obtained by mixing different numbers of human cells with a constant number of murine cells. In long-term experiments, cells (7×10^6 per mouse) were inoculated into the hind limb muscles of SCID-Beige inbred mice (five mice per group). Five weeks later, the mice were sacrificed for evaluation of the RMS cells present in blood, BM, liver, and lungs. Detection of human cells was performed as described above.

To study the effects of a pharmacological inhibition of S1P signaling on the metastasis of RMS in vivo, the lyophilized S1P-binding Spiegelmer NOX-S93 (synthesized at NOXXON Pharma AG, Berlin, Germany), a 44mer oligonucleotide conjugated to 40 kDa polyethylene glycol to increase circulation half-life was dissolved in 5% glucose and administered in summary seven times intraperitoneally, with the first dose of 20 mg/kg body weight (in 50 μl) every 12 hours starting 30 min after irradiation (750 cGy) to SCID/beige inbred mice. Control animals received 5% glucose only. 24 h after irradiation RMS cells were injected intravenously (i.v.; 3×10^6 per mouse). Bone marrow, liver and kidney were analyzed for the presence of RMS cells 48 h after injection (72 h after irradiation) by PCR as described above.

Quantitation of C1P and S1P by tandem mass spectrometry

Analysis of bioactive lipid content in tissue samples was performed on the frozen tissue organ samples. Frozen tissue was weighed and homogenized in methanol followed by lipid extraction using acidified organic solvents, as previously described (24). Analysis of S1P and C1P was carried out using a Shimadzu UFLC coupled with an AB Sciex 4000-Qtrap hybrid linear ion trap triple quadrupole mass spectrometer in multiple reaction monitoring (MRM) mode. Detailed LCMSMS conditions for analysis of S1P were previously described in Selim et al (25). Various C1P species were separated using an Agilent Zorbax Eclipse XDB C8 column, 5 μm, 4.6 × 150 mm column. The mobile phase consisted of 75/25 of methanol/water with formic acid (0.5%) and 5 mM ammonium formate (0.1%) as solvent A and 99/1of methanol/water with formic acid (0.5%) and 5 mM ammonium formate (0.1%) as solvent B. For the analysis of various C1P species the separation was achieved by maintaining 75% of solvent B for 3 min, then increasing to 100% B over the next 3 min and maintaining at 100% B for the last 18 minutes. Column is equilibrated back to the initial conditions in 3 min. The flow rate was 0.5 mL/min with a column temperature of 60 °C. The sample injection volume was 10 uL. The mass spectrometer was operated in the positive electrospray ionization mode with optimal ion source settings determined by synthetic standards with a declustering potential of 46 V, entrance potential of 10 V, collision energy of 19 V, collision cell exit potential of 14 V, curtain gas of 30 psi, ion spray voltage of 5500 V, ion source gas1/gas2 of 40 psi and temperature of 550 °C. MRM transitions monitored were as follows: 644.5/264.4 and 646.5/264.4 for C18-C1P.

Flow cytometric analysis of $S1PR_1$ expression

RH30-sh$S1PR_1$ and RH30-shRenilla cells were harvested at 50–60% confluence using CellStripper (Cellgro, Manassas, VA) then washed twice. Cells were stained against S1P receptor-1 (PE conjugated Abs, clone 218713 RnD Systems, Minneapolis, MN) and PE IgG isotype controls (RnD systems, Minneapolis, MN). Staining was performed in PBS with 2% fetal bovine serum (FBS, Invitrogen, Carlsbad, CA), at 4° C for 30 min. Cells were subsequently washed, re-suspended and analyzed using an LSR II (BD Biosciences). At least 2×10^6 events were acquired from each sample. FlowJo software was used for analysis (Tree Star, Ashland, OR).

Statistical Analysis

All results were presented as mean ± SD. Statistical analysis of the data was done using the nonparametric Mann-Whitney test (animal studies) and Student's t test (cell line experiments) for unpaired samples, with $p < 0.05$ considered significant.

Results

While S1P and C1P do not affect proliferation and survival of RMS cells, they strongly induce chemokinetic migration of these cells

Both S1P and C1P have been reported to stimulate proliferation of normal skeletal muscle cells (8, 26). To our surprise, however, neither S1P nor C1P affected proliferation of the RMS cell lines investigated in this study. Furthermore, they also did not enhance survival of RMS cells cultured in serum-free conditions (data not shown). By contrast, both bioactive lipids strongly enhanced robust migration of RMS cells (Figure 1).

The motility of cancer cells plays a crucial role in the process of tumor metastasis, and we have investigated the role of various chemokines and growth factors in the migration of RMS cells (4, 5, 27, 28). Figure 1A shows the migration of ARMS cells (RH30) in response to physiological doses of S1P and C1P present in biological fluids in comparison to gradients of α-chemokine stromal cell-derived factor-1 (SDF-1) and hepatocyte growth factor/scatter factor (HGF/SF), which, as we demonstrated, are potent chemoattractants for human RMS cells (4, 5). We found that at physiological doses, S1P and C1P increase migration of these cells, and the chemotactic response of RMS cells to a gradient of biological lipids was much higher than observed for physiological doses of SDF-1 and HGF/SF and comparable to optimal supra-physiological SDF-1 and HGF/SF doses. Interestingly, a dose-response migration assay (Figure 1B) revealed that RH30 cells respond robustly to both bioactive lipids employed at physiological doses, and increases in S1P and C1P concentrations in lower Transwell chambers inhibit migration. Figure 1C demonstrates that S1P and C1P are chemoattractants for 10 and 8 out of 10 different human RMS cell lines, respectively.

To address whether the observed increase in motility is a result of a chemotactic or a chemokinetic response (29), we performed a checkerboard assay in which S1P or C1P were added at the same time into the upper and the lower Transwell chambers. Figure 1D demonstrates that the migration of RH30 and RD cells was not significantly changed in these conditions, which indicates random chemokinetic rather than gradient-enforced chemotactic motility of RMS cells.

Human RMS cells express functional G protein-coupled S1P and C1P receptors

To address whether RMS cells express functional receptors for S1P and C1P, all 10 RMS cells lines were first made quiescent and then subsequently stimulated by S1P or C1P to see a potential effect on the phosphorylation of MAPK p42/44 and AKT (Figure 2A). These

signaling pathways have been selected because of their known role in migration and adhesion of normal (30, 31) and malignant cells (32, 33). We observed that five out of seven ARMS and two out of three ERMS cell lines responded robustly to S1P and C1P stimulation and, more importantly, the activation of MAPKp42/44 and/or AKT correlated with their migratory responsiveness (Figure 1C). Furthermore, while the chemokinetic responsiveness of RH30 cells (ARMS cell line) and RD cells (ERMS cell line) to S1P gradient was inhibited by MEK, AKT and $G_{\alpha i}$ protein inhibitors - UO126, MK2206 and pertussis toxin (PTx), respectively, the responsiveness of these cells to C1P was inhibited in the presence of the PI3K, AKT the $G_{\alpha i}$ protein inhibitory molecules - LY294002, MK2206 and PTx respectively (Figure 2B and Supplementary Figure 1). This confirms involvement MAPKp42/44 and/or AKT in S1P and C1P signaling. This latter observation suggests that while C1P receptor/s have not yet been identified, C1P signaling is PTx dependent and thus most likely involves G protein-coupled receptors. Furthermore, C1P signaling, in contrast to S1P, seems to be more sensitive to PI3 and AKT inhibition by LY294002 and MK2006, respectively.

In contrast to C1P receptor/s, five G protein-coupled receptors ($S1PR_{1–5}$) have been described and cloned. However, while RT-PCR revealed that most of the RMS cell lines express all five receptors (data not shown), we focused on the three most important: $S1PR_1$ and $S1PR_3$, which promote migration of several cell lines (34, 35), and $S1PR_2$, which has the opposite effect (35, 36). To unravel this complexity, we employed real-time quantitative PCR (qRT-PCR) to compare the relative expression among RMS cell lines (Figure 2C). We observed that whereas pro-migratory $S1PR_1$ and $S1PR_3$ were predominantly expressed in ARMS cell lines, migration-inhibiting $S1PR_2$ was highly expressed in ERMS cells.

To better understand the role of $S1PR_{1–3}$ in S1P-induced motility of RMS cells, we employed commercially available specific $S1PR_{1–3}$ inhibitors (Figure 2D) and found that inhibition of $S1PR_1$ and $S1PR_3$ receptors by W146 and BML-241, respectively, decreased motility of RH30 cells in the presence of S1P, whereas exposure of RH30 cells to the specific $S1PR_2$ antagonist JTE-012 lead even to a small increase in the number of migrating cells. By contrast, the migration of RD cells was only affected by inhibiting the $S1PR_3$ receptor (Figure 2D), which suggests that S1P-induced cell motility depends on $S1PR_1$ and $S1PR_3$ signaling and varies with cell line.

S1P and C1P increase adhesion of RMS cells and induce changes in the β-actin cytoskeleton

Another important feature of metastasizing cancer cells is their adhesiveness at the site of metastasis. Therefore, we next evaluated the adhesion of RMS cell lines to fibronectin-covered dishes and to a bone marrow stromal cell monolayer. We found that both bioactive lipids strongly induce adhesion of RMS cells to fibronectin in a dose-responsive manner (Figure 3A) and that S1P, but not C1P, also strongly enhances adhesion of RH30 and RD cells to BM-derived stroma (Figure 3B). However, while we noticed that an increase in C1P dose resulted in more robust adhesion to fibronectin (Figure 3A) an increase in a dose of this bioactive lipid had in contrast slightly opposite effect on cell migration (Figure 1B).

It is well known that the dynamic reorganization of the cytoskeleton is a necessary step for cell adhesion and migration. Thus, we examined the β-actin cytoskeleton organization and the localization of the focal adhesion-associated protein paxillin by employing confocal microscope analysis in S1P- or C1P-stimulated and non-stimulated RH30 and RD cells (Figure 3C). We observed that RMS cells placed in control medium display well-developed bundles of F-actin arranged parallel to the long axis of cells, with paxillin mainly present in the cytoplasm. By contrast, in response to S1P or C1P, the β-actin cytoskeleton became reorganized toward the leading edge of the cell. Furthermore, in stimulated cells, paxillin

was translocated close to the cell membrane at focal adhesion sites. These data confirm that both bioactive lipids increase adhesion of RMS cells.

The effect of $S1PR_1$ downregulation on *in vivo* tumor growth of RH30 cells

To assess the role of S1P in the metastasis of RMS cells, we downregulated the $S1PR_1$ receptor in RH30 cells by employing an shRNA strategy that reduced $S1PR_1$ expression by ~75% (Figure 4A). RH30 cells were selected for this study based on their robust S1P-mediated motility (Figure 1) and because this responsiveness was strongly affected by the presence of the $S1PR_1$ small-molecule inhibitor W146 (Figure 2D). Additional FACS analysis performed on $shS1PR_1$ transfected RH30 cells revealed decrease in $S1PR_1$ expression by ~ 85% (Figure 4B). Of note, we did not observed significant differences in proliferation or apoptosis ratio between $shS1PR_1$ and shRenilla RH30 cells (data not shown).

Figure 4C shows that downregulation of $S1PR_1$ in RH30-$shS1PR_1$ cells severely reduced the responsiveness of these cells to S1P, however their response to C1P remain unchanged. In the next step, to test the effect of $S1PR_1$ downregulation on metastatic behavior of RH30 cells, we inoculated RH30-shRenilla (control) and RH30-$shS1PR_1$ cells into the femoral muscles of SCID/beige mice and observed that RH30-$shS1PR_1$ cells formed significantly smaller tumors compared with control RH30-shRenilla cells (Figure 4D). Furthermore, 5 weeks after inoculation of RMS cells, we observed a lower number of RH30-$shS1PR_1$ cells in BM, lungs, as well as in liver and circulating peripheral blood (Figure 4E), which clearly demonstrates involvement of the S1P–$S1PR_1$ axis in RMS metastasis in vivo.

Irradiation and chemotherapy increase S1P and C1P levels in bone marrow

We have proposed that one of the unwanted side effects of radio/chemotherapy is induction of a pro-metastatic environment in different tissues (18). To see whether radio/chemotherapy may in fact increase S1P and C1P levels in different organs, S1P and C1P levels were measured in supernatants harvested from murine BM, liver, brain, and lungs, which are frequent sites of RMS metastasis before and after treatment, by employing a sensitive mass spectrometry-based approach. We observed that the concentrations of S1P and C1P increased predominantly in irradiated BM, but also in irradiated liver, and lungs (Supplementary Figure 2) as well as in supernatants harvested from cell suspensions prepared from these organs (data not shown).

To test whether supernatants form these organs induce motility of RMS cells, we tested the responsiveness of RH30 cells in the Transwell migration assay and found that RH30 cells respond robustly to these supernatants (Figure 5A). We were aware that such CM contain several potential chemotactic factors, and thus to assess the importance of the contribution by S1P, we repeated these migratory assays with control RH30-shRenilla and RH30-$shS1PR_1$ cell lines. Figure 5B demonstrates that the response to CM harvested from irradiated BM, liver, and lungs was affected by downregulation of $S1PR_1$ on RH30 cells, which suggests a significant contribution by the S1P–$S1PR_1$ axis. The prometastatic involvement of S1P in RMS metastasis has been evaluated by employing two different approaches to increase in vivo S1P level in the tissues (irradiation or exposure to DOP). As it is shown in Figure 5C in both experimental models we observed increased number of RH30 cells in murine organs after intravenous injection of RH30 cells, and this effect was $S1PR_1$ mediated.

In a similar type of experiment, we evaluated the effect of chemotherapy on induction of a pro-metastatic microenvironment. Supplementary Figure 3A shows an increase in S1P and C1P levels in the BM of mice treated with vincristine, which is the most common cytostatic

agent employed in chemotherapy protocols for RMS (37). CM harvested from BM of mice treated with vincristine induced increased motility activity of RH30 cells (Supplementary Figure 3B), which again was reduced if RH30-shS1PR$_1$ cells were employed in the Transwell migration assay (Supplementary Figure 3C).

Spiegelmer NOX-S93 inhibits S1P-dependent migration of RMS cells

Finally, we modulated the unwanted in vivo S1P-induced motility of RMS cells by employing the anti-S1P Spiegelmer NOX-S93 that prevents S1P binding to its receptors (unpublished data, manuscript in preparation). As mentioned above Spiegelmers are biostable and immunologically passive mirror-image (L-stereoisomer) oligonucleotides that can be identified to bind to pharmacologically relevant targets with high affinity and specificity.

Figure 6A shows that NOX-S93 inhibits dose-dependently the pro-migratory activity of RH30-shRenilla, but not RH30-shS1PR$_1$ cells, to BM extracts that were irradiated with 1500 cGy. The selective inhibitory effect of NOX-S93-pretreated BM supernatants against S1PR$_1$-expressing RH30-shRenilla cells demonstrates a selective effect of this anti-S1P compound on the S1P–S1PR$_1$ axis.

Finally, to check whether NOX-S93 inhibits the S1P-dependent spread of RMS cells to tissues damaged by irradiation in vivo, we compared the seeding efficiency to different organs (BM, lungs, and liver) of RH30 cells injected into control non-irradiated and 750-cGy-irradiated SCID/beige mice (Figure 6B). We found that the irradiation-increased seeding efficiency of RH30 cells, especially into BM, was significantly reduced after administration of NOX-S93. This corroborates the observation that the S1P level is highly elevated in irradiated BM (Supplementary Figure 2).

Discussion

Two major problems in cancer therapy are the recurrence of tumor growth after successful initial treatment and the fatal tendency of cancerous cells to spread and metastasize to different vital organs (38, 39). The ability to metastasize is one characteristic of highly malignant and primitive tumors including RMS (2), and different tumors often have preferred organs to which they metastasize (39). The tropism of cancer cells to metastasize to selected organs pinpoints the involvement of organ-specific factors that direct metastasis (40). These factors may promote the formation of a pre-metastatic niche that provides metastasizing tumor cells a favorable growth and survival environment. In support of this notion, we have demonstrated an important role of the α-chemokine stromal derived factor-1 (SDF-1)–CXCR4 axis in metastasis of RMS cells to BM, which is one of the common metastatic sites for RMS cells (2).

As with other cancer types, the metastasis of RMS cells is directed by several growth factors, including HGF/SF (5), IGF-1 (41), and several chemokines such as SDF-1 (4), interferon-inducible T-cell alpha chemoattractant (I-TAC) (22), and macrophage migration inhibitory factor (MIF) (28). However, in addition to these pro-metastatic, peptide-based factors, evidence has accumulated that a family of bioactive lipids plays an important and underappreciated role (42). In particular, S1P has been demonstrated to be involved in metastasis of lung (10), breast (11), prostate (43), and liver (12) cancer cells. In contrast to S1P, there are no reports of the involvement of another bioactive lipid, C1P, in cancer metastasis. However, C1P, as reported by others and us, is a potent modulator of the trafficking of monocytes (15), hematopoietic stem progenitor cells (44), mesenchymal stromal cells (17), endothelial progenitors (17), and murine myoblasts (8). Similarly, S1P has also been proposed to play an important role in trafficking of non-malignant cells such

as hematopoietic stem progenitor cells (6, 44), mesenchymal stromal cells (45), and endothelial progenitors (17). It thus plays a role in skeletal muscle development (46), angiogenesis (47), and tissue regeneration from injury (9) and acts directly on skeletal muscle satellite stem cells (26).

The effects of S1P and C1P in myogenesis (8, 46) could be relevant to the effect on RMS proliferation. However, we did not observe any effect of either bioactive lipid on proliferation or survival of RMS cells. Nevertheless, our data showing an effect of S1P and C1P on trafficking of RMS cells corroborates their effect in modulating the trafficking of normal skeletal muscle-derived cells (26).

The metastasis of a tumor is a multi-step process, and in the first step, cells endowed with a higher motility potential detach from the primary tumor mass and migrate into the peripheral blood, lymph vessels, or internal body cavities. In this process, we distinguish two major types of cell motility: chemotaxis, (directed migration to the gradient) and chemokinesis (random migration of cells in response to a chemoattractant). While the first type of motility may explain tropism of cancer cells to a particular organ that is a source of specific chemoattractant, the other type of motility reflects the ability of tumor cells to detach from the primary tumor in a search for a new environment where they can grow and expand. However, these processes are tightly connected and together result in tumor metastatic growth.

In this paper, by employing a checkerboard migration assay (Figure 1D), we demonstrate for the first time that the roles of bioactive phospholipids S1P and C1P are mainly in inducing random chemokinetic migration of RMS cells. It would be interesting to see whether this type of motility is also involved in metastasis of other types of cancer cells (e.g., lung, breast, or prostate). However, it is worth mentioning that, in contrast to RMS cells, we have already excluded chemokinesis in S1P- and C1P-induced migration of normal hematopoietic cells (44), mesenchymal stromal cells (17), and endothelial progenitors (17). This suggests that differences in migratory responsiveness to bioactive lipid gradients may exist between normal and malignant cells.

One of the most important observations in this current work is that RMS cells respond to S1P and C1P at doses normally encountered in peripheral blood and lymph. Thus, we can envision a scenario that, while S1P and C1P are involved in increasing overall motility of RMS cells and promote their egress from the primary tumor, other factors such as SDF-1 or HGF/SF tune and direct their final migration to distant places that secrete high levels of these chemoattractants (e.g. SDF-1-directed metastasis into the BM microenvironment and lymph nodes) (4).

By employing small molecule antagonists to the S1P receptor and shRNA-based receptor knockdown experiments, we have demonstrated that, as reported for other cell types, $S1PR_1$ and $S1PR_2$ play an important role in modulating RMS cell migration and adhesion. While the C1P receptor has not yet been identified, our migration studies in the presence of S1P antagonists and signaling studies in the presence of specific signaling inhibitors (Figure 2B and D) have confirmed that the C1P receptor is most likely a G protein-coupled, PTX-sensitive receptor that is distinct from S1P receptors (15).

A basic clinical problem is the recurrence of metastatic tumors after radio/chemotherapy (18, 48). The reason for this is the presence of therapy-resistant tumor cells that survive at the primary tumor site or in already established sites of micro-metastases. On the other hand, it is known that radio/chemotherapy delivers a toxic insult to the tissues that may result in induction of a pro-metastatic microenvironment (18, 19). In support of this notion, we have already shown that two important RMS pro-metastatic factors, SDF-1 and HGF/SF, are

upregulated at the mRNA level in irradiated BM (44). In this current report, we show that radio/chemotherapy may also induce bioactive lipids in the BM microenvironment as well as in other tissues. Thus, the induction of a pro-metastatic microenvironment in peripheral tissues may create permissive conditions for tumor cells that survive treatment to lodge and expand, and S1P could here play an important role.

There are several strategies under development for modulating the S1P–$S1PR_1$ receptor axis to inhibit in vivo cancer expansion, including sphingosine kinase inhibitors (49), anti-S1P blocking antibodies (50), and the novel oligonucleotide-based Spiegelmer NOX-S93. In our work to better address the role of radio/chemotherapy-induced S1P, we have employed NOX-S93 to block the chemotactic S1P level in circulating blood and peripheral tissues in irradiated mice. We found that S1P released from irradiated or chemotherapy-damaged tissues was efficiently blocked by this chemical entity leading to inhibition of RMS cell migration mediated by the S1P–$S1PR_1$ axis. The effect on BM metastasis was most prominent probably due to the fact that S1P levels increase much stronger in BM than in lung and liver where other chemotactic modulators may play a more important role. We envision that this inhibition of metastasis could be even more efficient when combining anti-S1P Spiegelmers with similar molecules targeted against C1P and SDF-1, and we are currently testing appropriate compounds in in vivo models.

In summary, our data for the first time demonstrate that S1P and C1P already present at physiological concentrations in peripheral blood or lymph induce pro-metastatic phenotype of RMS cells. We also demonstrate that both of these bioactive lipids become upregulated in tissues exposed to radio/chemotherapy and thus contribute to a pro-metastatic microenvironment in several organs including BM (Figure 6C). The radiotherapy-induced spread of RMS cells can be efficiently inhibited in vivo after neutralizing circulating S1P, and compounds such as the anti-S1P Spiegelmer NOX-S93 could play an important clinical role in preventing RMS metastasis. Finally we are aware that our data performed with established RMS cell lines, needs further conformation with cells isolated from primary RMS tumors.

Supplementary Material

Refer to Web version on PubMed Central for supplementary material.

Acknowledgments

This work was supported by NIH grant 2R01 DK074720,1R01HL112788-01A1, the Stella and Henry Endowment, the European Union structural funds (Innovative Economy Operational Program POIG.01.01.02-00-109/09-00) and grant Maestro 2011/02/A/NZ4/00035 to MZR. The authors wish to thank the NOXXON chemistry group (John Turner, Lucas Bethge) for synthesis of NOX-S93 and Dirk Zboralski for helpful discussions.

References

1. Collins MH, Zhao H, Womer RB, Barr FG. Proliferative and apoptotic differences between alveolar rhabdomyosarcoma subtypes: a comparative study of tumors containing PAX3-FKHR or PAX7-FKHR gene fusions. Med Pediatr Oncol. 2001; 37(2):83–9. [PubMed: 11496344]
2. Sandberg AA, Stone JF, Czarnecki L, Cohen JD. Hematologic masquerade of rhabdomyosarcoma. Am J Hematol. 2001; 68(1):51–7. [PubMed: 11559937]
3. Davis RJ, D'Cruz CM, Lovell MA, Biegel JA, Barr FG. Fusion of PAX7 to FKHR by the variant t(1;13)(p36;q14) translocation in alveolar rhabdomyosarcoma. Cancer Res. 1994; 54(11):2869–72. [PubMed: 8187070]

4. Libura J, Drukala J, Majka M, Tomescu O, Navenot JM, Kucia M, et al. CXCR4-SDF-1 signaling is active in rhabdomyosarcoma cells and regulates locomotion, chemotaxis, and adhesion. Blood. 2002; 100(7):2597–606. [PubMed: 12239174]
5. Jankowski K, Kucia M, Wysoczynski M, Reca R, Zhao D, Trzyna E, et al. Both hepatocyte growth factor (HGF) and stromal-derived factor-1 regulate the metastatic behavior of human rhabdomyosarcoma cells, but only HGF enhances their resistance to radiochemotherapy. Cancer Res. 2003; 63(22):7926–35. [PubMed: 14633723]
6. Ratajczak MZ, Lee H, Wysoczynski M, Wan W, Marlicz W, Laughlin MJ, et al. Novel insight into stem cell mobilization-plasma sphingosine-1-phosphate is a major chemoattractant that directs the egress of hematopoietic stem progenitor cells from the bone marrow and its level in peripheral blood increases during mobilization due to activation of complement cascade/membrane attack complex. Leukemia. 2010; 24(5):976–85. [PubMed: 20357827]
7. Kimura F, Miyazaki M, Suwa T, Sugiura T, Shinoda T, Itoh H, et al. Plasma human hepatocyte growth factor concentrations in patients with biliary obstruction. J Gastroenterol Hepatol. 2000; 15(1):76–82. [PubMed: 10719751]
8. Gangoiti P, Bernacchioni C, Donati C, Cencetti F, Ouro A, Gomez-Munoz A, et al. Ceramide 1-phosphate stimulates proliferation of C2C12 myoblasts. Biochimie. 2012; 94(3):597–607. [PubMed: 21945811]
9. Germinario E, Peron S, Toniolo L, Betto R, Cencetti F, Donati C, et al. S1P2 Receptor Promotes Mouse Skeletal Muscle Regeneration. J Appl Physiol. 2012; 113(5):707–13. [PubMed: 22744969]
10. Hsu A, Zhang W, Lee JF, An J, Ekambaram P, Liu J, et al. Sphingosine-1-phosphate receptor-3 signaling up-regulates epidermal growth factor receptor and enhances epidermal growth factor receptor-mediated carcinogenic activities in cultured lung adenocarcinoma cells. Int J Oncol. 2012; 40(5):1619–26. [PubMed: 22344462]
11. Kim ES, Kim JS, Kim SG, Hwang S, Lee CH, Moon A. Sphingosine 1-phosphate regulates matrix metalloproteinase-9 expression and breast cell invasion through S1P3-Galphaq coupling. J Cell Sci. 2011; 124(Pt 13):2220–30. [PubMed: 21652634]
12. Bao M, Chen Z, Xu Y, Zhao Y, Zha R, Huang S, et al. Sphingosine kinase 1 promotes tumour cell migration and invasion via the S1P/EDG1 axis in hepatocellular carcinoma. Liver Int. 2012; 32(2): 331–8. [PubMed: 22098666]
13. Hammad SM, Pierce JS, Soodavar F, Smith KJ, Al Gadban MM, Rembiesa B, et al. Blood sphingolipidomics in healthy humans: impact of sample collection methodology. J Lipid Res. 2010; 51(10):3074–87. [PubMed: 20660127]
14. Ratajczak MZ, Kim C, Wu W, Shin DM, Bryndza E, Kucia M, et al. The role of innate immunity in trafficking of hematopoietic stem cells-an emerging link between activation of complement cascade and chemotactic gradients of bioactive sphingolipids. Adv Exp Med Biol. 2012; 946:37–54. [PubMed: 21948361]
15. Granado MH, Gangoiti P, Ouro A, Arana L, Gonzalez M, Trueba M, et al. Ceramide 1-phosphate (C1P) promotes cell migration Involvement of a specific C1P receptor. Cell Signal. 2009; 21(3): 405–12. [PubMed: 19041940]
16. Kluk MJ, Hla T. Signaling of sphingosine-1-phosphate via the S1P/EDG-family of G-protein-coupled receptors. Biochim Biophys Acta. 2002; 1582(1–3):72–80. [PubMed: 12069812]
17. Kim C, Abdel-Latif A, Mierzejewska K, Schneider G, Sunkara M, Ratajczak J, et al. Ceramide-1-phosphate regulates migration of multipotent stromal cells (MSCs) and endothelial progenitor cells (EPCs) – implications for tissue regeneration. Stem Cells. 201210.1002/stem.1291
18. Ratajczak M, Tarnowski M, Staniszewska M, Sroczynski T, Banach B. Mechanisms of cancer metastasis: involvement of cancer stem cells? Minerva Med. 2010; 101(3):179–91. [PubMed: 20562805]
19. Park SI, Liao J, Berry JE, Li X, Koh AJ, Michalski ME, et al. Cyclophosphamide creates a receptive microenvironment for prostate cancer skeletal metastasis. Cancer Res. 2012; 72(10): 2522–32. [PubMed: 22589273]
20. Ulrich H, Trujillo CA, Nery AA, Alves JM, Majumder P, Resende RR, et al. DNA and RNA aptamers: from tools for basic research towards therapeutic applications. Comb Chem High Throughput Screen. 2006; 9(8):619–32. [PubMed: 17017882]

21. [cited; Available from: http://www.clinicaltrials.gov
22. Grymula K, Tarnowski M, Wysoczynski M, Drukala J, Barr FG, Ratajczak J, et al. Overlapping and distinct role of CXCR7-SDF-1/ITAC and CXCR4-SDF-1 axes in regulating metastatic behavior of human rhabdomyosarcomas. Int J Cancer. 2010; 127(11):2554–68. [PubMed: 20162608]
23. Gomes C, Smith SC, Youssef MN, Zheng JJ, Hagg T, Hetman M. RNA polymerase 1-driven transcription as a mediator of BDNF-induced neurite outgrowth. J Biol Chem. 2011; 286(6):4357–63. [PubMed: 21098478]
24. Mathews TP, Kennedy AJ, Kharel Y, Kennedy PC, Nicoara O, Sunkara M, et al. Discovery, biological evaluation, and structure-activity relationship of amidine based sphingosine kinase inhibitors. J Med Chem. 2010; 53(7):2766–78. [PubMed: 20205392]
25. Selim S, Sunkara M, Salous AK, Leung SW, Berdyshev EV, Bailey A, et al. Plasma levels of sphingosine 1-phosphate are strongly correlated with haematocrit, but variably restored by red blood cell transfusions. Clin Sci (Lond). 2011; 121(12):565–72. [PubMed: 21749329]
26. Calise S, Blescia S, Cencetti F, Bernacchioni C, Donati C, Bruni P. Sphingosine 1-phosphate stimulates proliferation and migration of satellite cells: role of S1P receptors. Biochim Biophys Acta. 2012; 1823(2):439–50. [PubMed: 22178384]
27. Wysoczynski M, Miekus K, Jankowski K, Wanzeck J, Bertolone S, Janowska-Wieczorek A, et al. Leukemia inhibitory factor: a newly identified metastatic factor in rhabdomyosarcomas. Cancer Res. 2007; 67(5):2131–40. [PubMed: 17332343]
28. Tarnowski M, Grymula K, Liu R, Tarnowska J, Drukala J, Ratajczak J, et al. Macrophage migration inhibitory factor is secreted by rhabdomyosarcoma cells, modulates tumor metastasis by binding to CXCR4 and CXCR7 receptors and inhibits recruitment of cancer-associated fibroblasts. Mol Cancer Res. 2010; 8(10):1328–43. [PubMed: 20861157]
29. Tchou-Wong KM, Fok SY, Rubin JS, Pixley F, Condeelis J, Braet F, et al. Rapid chemokinetic movement and the invasive potential of lung cancer cells; a functional molecular study. BMC Cancer. 2006; 6:151. [PubMed: 16756685]
30. Yuan L, Hu J, Luo Y, Liu Q, Li T, Parish CR, et al. Upregulation of heparanase in high-glucose-treated endothelial cells promotes endothelial cell migration and proliferation and correlates with Akt and extracellular-signal-regulated kinase phosphorylation. Mol Vis. 2012; 18:1684–95. [PubMed: 22773906]
31. Shi Y, Xia YY, Wang L, Liu R, Khoo KS, Feng ZW. Neural cell adhesion molecule modulates mesenchymal stromal cell migration via activation of MAPK/ERK signaling. Exp Cell Res. 2012; 318(17):2257–67. [PubMed: 22683856]
32. Kim D, Kim S, Koh H, Yoon SO, Chung AS, Cho KS, et al. Akt/PKB promotes cancer cell invasion via increased motility and metalloproteinase production. Faseb J. 2001; 15(11):1953–62. [PubMed: 11532975]
33. Kukreja P, Abdel-Mageed AB, Mondal D, Liu K, Agrawal KC. Up-regulation of CXCR4 expression in PC-3 cells by stromal-derived factor-1alpha (CXCL12) increases endothelial adhesion and transendothelial migration: role of MEK/ERK signaling pathway-dependent NF-kappaB activation. Cancer Res. 2005; 65(21):9891–8. [PubMed: 16267013]
34. Yamashita H, Kitayama J, Shida D, Yamaguchi H, Mori K, Osada M, et al. Sphingosine 1-phosphate receptor expression profile in human gastric cancer cells: differential regulation on the migration and proliferation. J Surg Res. 2006; 130(1):80–7. [PubMed: 16183075]
35. Balthasar S, Samulin J, Ahlgren H, Bergelin N, Lundqvist M, Toescu EC, et al. Sphingosine 1-phosphate receptor expression profile and regulation of migration in human thyroid cancer cells. Biochem J. 2006; 398(3):547–56. [PubMed: 16753042]
36. Arikawa K, Takuwa N, Yamaguchi H, Sugimoto N, Kitayama J, Nagawa H, et al. Ligand-dependent inhibition of B16 melanoma cell migration and invasion via endogenous S1P2 G protein-coupled receptor. Requirement of inhibition of cellular RAC activity. J Biol Chem. 2003; 278(35):32841–51. [PubMed: 12810709]
37. Ruymann FB. The development of VAC chemotherapy in rhabdomyosarcoma: what does one do for an encore? Curr Oncol Rep. 2003; 5(6):505–9. [PubMed: 14521810]

38. Sethi N, Kang Y. Unravelling the complexity of metastasis - molecular understanding and targeted therapies. Nat Rev Cancer. 2011; 11(10):735–48. [PubMed: 21941285]
39. Nguyen DX, Bos PD, Massague J. Metastasis: from dissemination to organ-specific colonization. Nat Rev Cancer. 2009; 9(4):274–84. [PubMed: 19308067]
40. Zlotnik A, Burkhardt AM, Homey B. Homeostatic chemokine receptors and organ-specific metastasis. Nat Rev Immunol. 2011; 11(9):597–606. [PubMed: 21866172]
41. Kalebic T, Tsokos M, Helman LJ. In vivo treatment with antibody against IGF-1 receptor suppresses growth of human rhabdomyosarcoma and down-regulates p34cdc2. Cancer Res. 1994; 54(21):5531–4. [PubMed: 7923191]
42. Gangoiti P, Granado MH, Alonso A, Goni FM, Gomez-Munoz A. Implication of ceramide, ceramide 1-phosphate and sphingosine 1-phosphate in tumorigenesis. Transl Oncogenomics. 2008; 3:81–98. [PubMed: 21566746]
43. Sekine Y, Suzuki K, Remaley AT. HDL and sphingosine-1-phosphate activate stat3 in prostate cancer DU145 cells via ERK1/2 and S1P receptors, and promote cell migration and invasion. Prostate. 2011; 71(7):690–9. [PubMed: 20979115]
44. Kim CH, Wu W, Wysoczynski M, Abdel-Latif A, Sunkara M, Morris A, et al. Conditioning for hematopoietic transplantation activates the complement cascade and induces a proteolytic environment in bone marrow: a novel role for bioactive lipids and soluble C5b-C9 as homing factors. Leukemia. 2012; 26(1):106–16. [PubMed: 21769103]
45. Li C, Kong Y, Wang H, Wang S, Yu H, Liu X, et al. Homing of bone marrow mesenchymal stem cells mediated by sphingosine 1-phosphate contributes to liver fibrosis. J Hepatol. 2009; 50(6): 1174–83. [PubMed: 19398237]
46. Meacci E, Bini F, Sassoli C, Martinesi M, Squecco R, Chellini F, et al. Functional interaction between TRPC1 channel and connexin-43 protein: a novel pathway underlying S1P action on skeletal myogenesis. Cell Mol Life Sci. 2010; 67(24):4269–85. [PubMed: 20614160]
47. Takuwa Y, Du W, Qi X, Okamoto Y, Takuwa N, Yoshioka K. Roles of sphingosine-1-phosphate signaling in angiogenesis. World J Biol Chem. 2010; 1(10):298–306. [PubMed: 21537463]
48. Huang SH, Perez-Ordonez B, Weinreb I, Hope A, Massey C, Waldron JN, et al. Natural course of distant metastases following radiotherapy or chemoradiotherapy in HPV-related oropharyngeal cancer. Oral Oncol. 2013; 49(1):79–85. [PubMed: 22917550]
49. Kotelevets N, Fabbro D, Huwiler A, Zangemeister-Wittke U. Targeting Sphingosine Kinase 1 in Carcinoma Cells Decreases Proliferation and Survival by Compromising PKC Activity and Cytokinesis. PLoS One. 2012; 7(6):e39209. [PubMed: 22761740]
50. Sabbadini RA. Sphingosine-1-phosphate antibodies as potential agents in the treatment of cancer and age-related macular degeneration. Br J Pharmacol. 2011; 162(6):1225–38. [PubMed: 21091645]

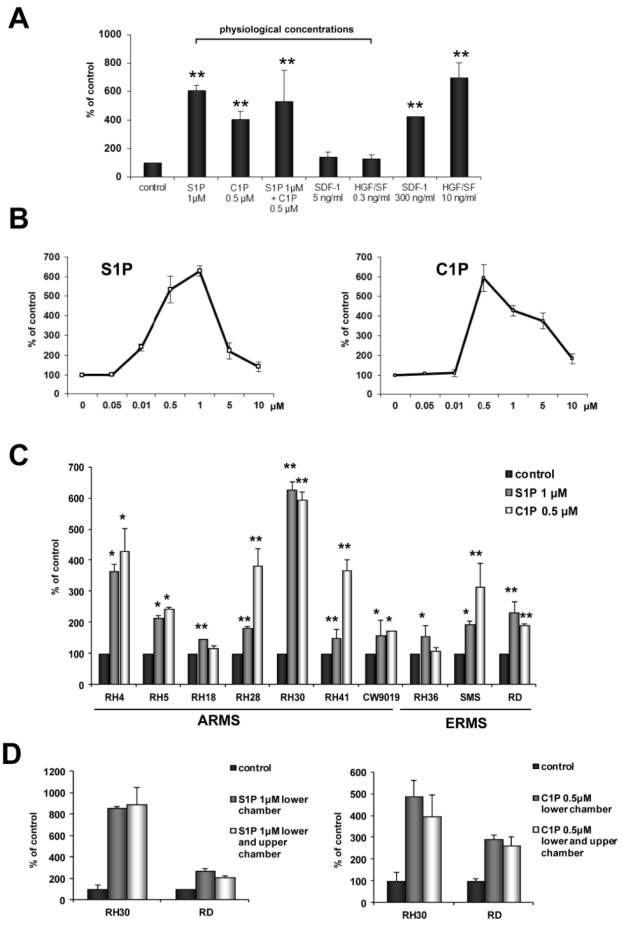

Figure 1. Bioactive lipids S1P and C1P are chemoattractants for RMS cells at concentrations corresponding to physiological concentrations in plasma

Panel A - Chemotaxis of RH30 cells in response to S1P (1 μM, considered as physiological dose (13)), C1P (0.5 μM, considered as physiological dose (13)), SDF1 (5 or 300 ng/ml), and HGF (0.3 or 10 ng/ml). Data are pooled from three independent experiments. **Panel B** - Dose-dependent effect of S1P and C1P on migration of RH30. **Panel C** - Chemotaxis of different RMS cell lines across transwell membranes in response to S1P (1 μM) or C1P (0.5 μM). **Panel D** -Chemotaxis and chemokinesis of RH30 and RD cells in response to S1P (1 μM) and C1P (0.5 μM). The chemotaxis assay was done at least twice in duplicate, with similar results. Results are presented as means +/− SD, with a statistical significance relative to the control of *$p < 0.05$ and **$p < 0.01$.

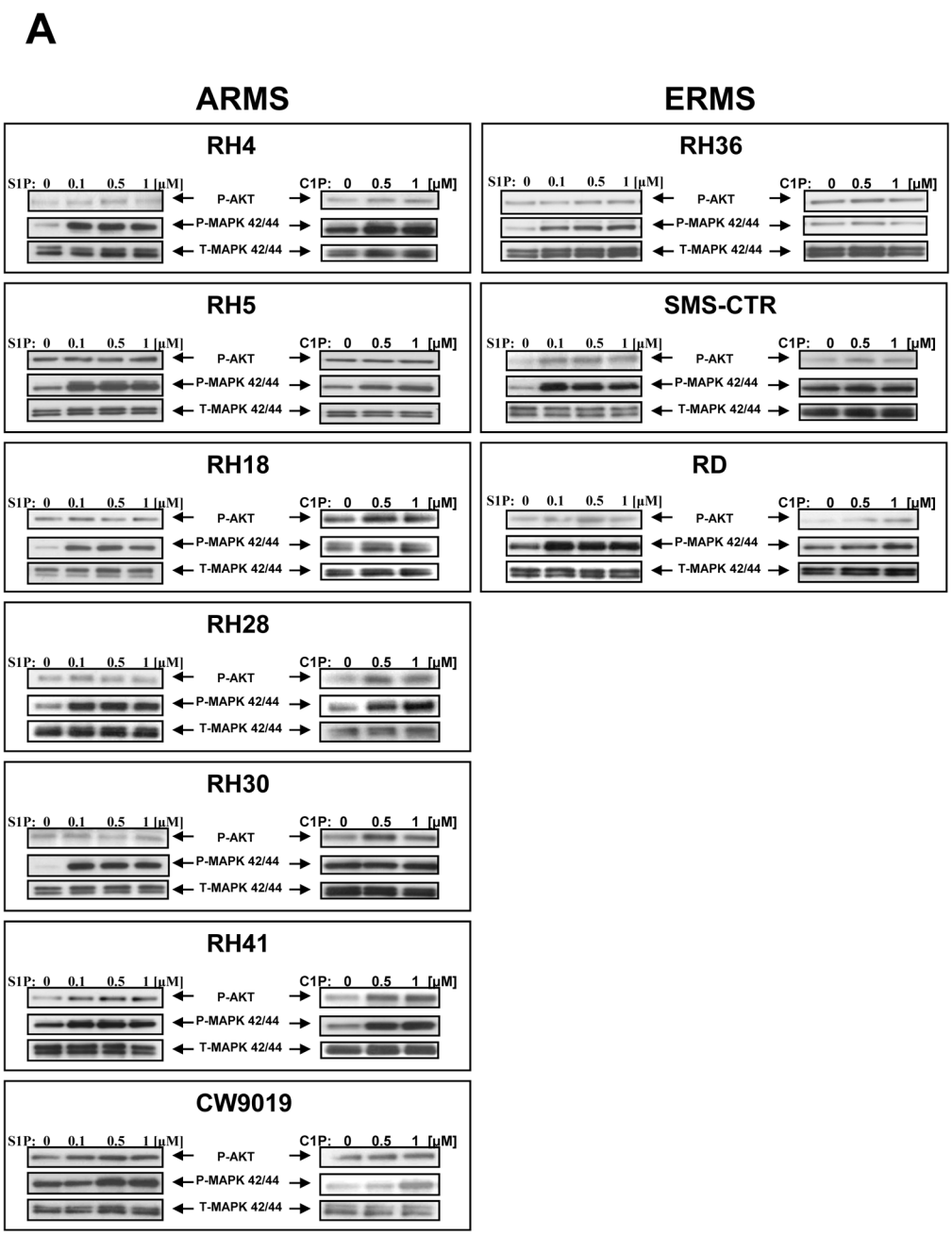

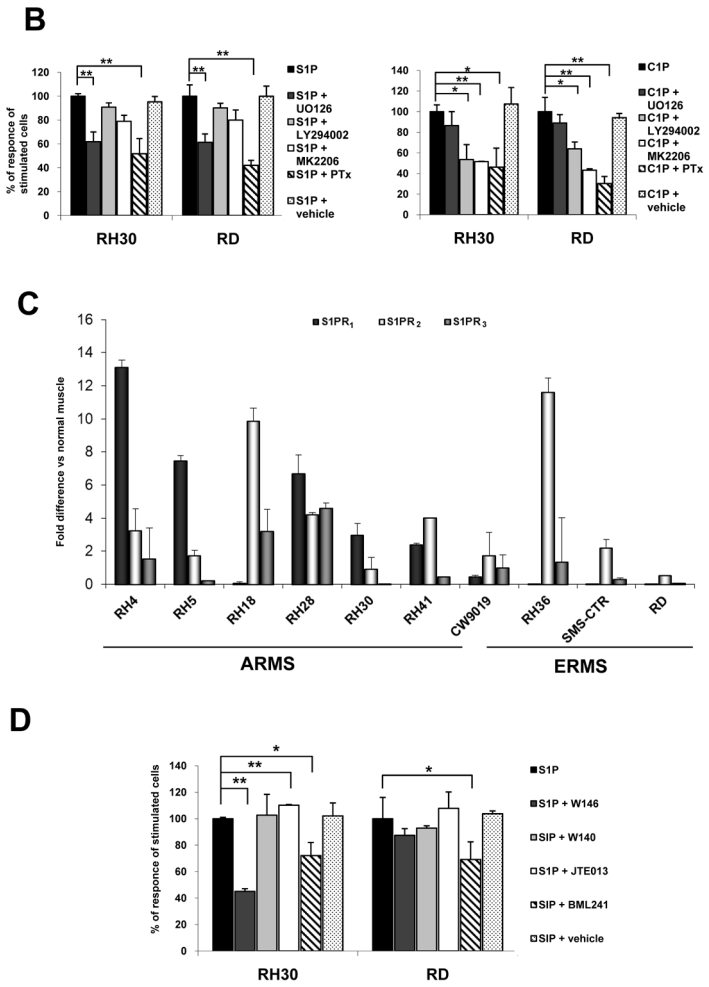

Figure 2. S1P and C1P activate MAPK and AKT intracellular pathway proteins and induce migration of human RMS cell lines through G protein-coupled receptors

Panel A - Phosphorylation of MAPK p42/44 and AKT in human RMS cell lines stimulated for 5 min by S1P (0.1, 0.5, or 1 μM) or C1P (0.5 or 1 μM). The experiment was repeated three times with similar results, and a representative study is shown. **Panel B –** The effect of LY294002, UO126, MK2206 and pertusis toxin (PTX) or vehicle alone on the migration of RH30 and RD cells in response to S1P (1 μM) or C1P (0.5 μM). The experiment was done twice with similar results. *$p < 0.05$ or **$p < 0.01$ indicates statistical significance relative to the control (cells migrating in response to S1P or C1P alone). **Panel C –** qRT-PCR for $S1PR_{1–3}$ revealed differences in expression of these receptors between ARMS and ERMS cell lines. The experiment was repeated twice on two different batches of cells, with similar results. **Panel D -** Chemotaxis of RMS cell lines to S1P (1 μM) in the absence or presence of the S1PR1 inhibitor W146, the S1PR2 inhibitor JTE-013, or the S1PR3 inhibitor BML241. Chemotaxis of cells in the presence of vehicle or inactive analog of W146 – W140 are also presented. The results from two independent experiments are shown as means ± SD. *$p < 0.05$ or **$p < 0.01$ compared with the control (cells stimulated with S1P alone).

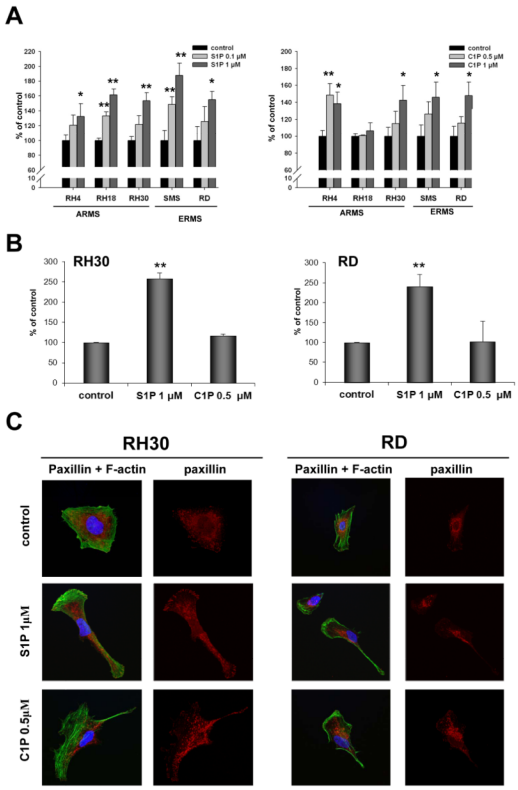

Figure 3. S1P and C1P increase the adhesivness of RMS cells and induce F-actin formation and translocation of paxillin to focal adhesion sites

Panel A - Adhesion of RMS cells to fibronectin. The cells were not stimulated (control) or stimulated with S1P (0.1 or 1 μM) or C1P (0.5 or 1 μM) for 1 h. The number of adherent cells was measured by microscopic analysis. Data from three separate experiments are pooled together and means ± SD are shown. *$p < 0.05$ and **$p < 0.01$ compared with the control. **Panel B -** Adhesion of RH30 and RD cells to mouse stromal cells. RMS cells stained with calcein were stimulated with S1P (1 μM) or C1P (0.5 μM) for 1 h. After a 15-minute incubation, non-adherent cells were removed and adherent cells counted under a fluorescent microscope. **Panel C -** Actin cytoskeleton organization and paxillin localization in RH30 and RD cells in medium alone or after 4-h stimulation with 1 μM S1P or 0.5 μM C1P. Representative images are shown.

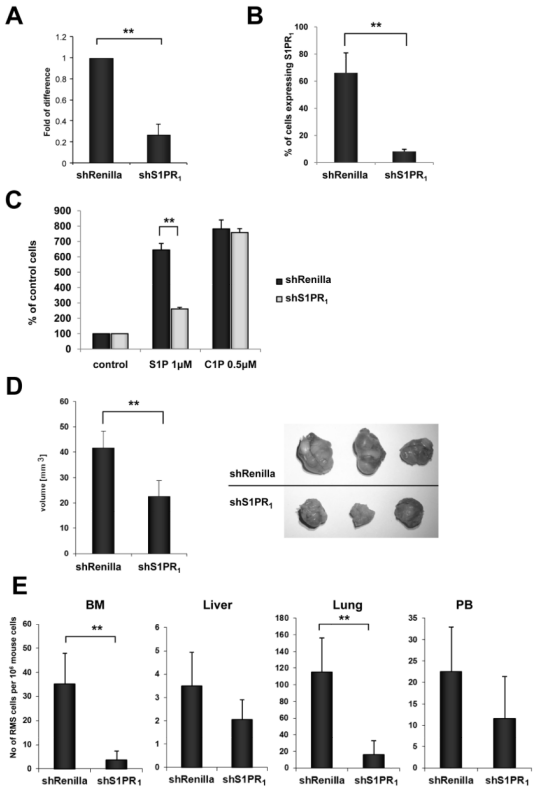

Figure 4. Downregulation of $S1PR_1$ inhibits RH30 cell growth *in vivo* and in metastasis

Panel A - qRT-PCR for $S1PR_1$ in RH30 cells transfected with plasmids encoding shRNA against Renilla (control) and against $S1PR_1$. The experiment was repeated twice on three different batches of cells with similar results. **$p < 0.01$. **Panel B** – FACS analysis of $S1PR_1$ expression in RH30-shRenilla and RH30-sh$S1PR_1$ cells. The experiment was repeated three times with similar results. **$p < 0.01$. **Panel C** - Chemotaxis of RH30 cells transfected with plasmid encoding shRNA against Renilla (control) and against $S1PR_1$ across Transwell membranes in response to S1P (1 μM). The results from three independent experiments are shown as means ± SD. *$p < 0.05$ or **$p < 0.01$ compared with the control. **Panel D -** RH30 tumor formation after downregulating $S1PR_1$ expression. Tumor formation by RH30-shRenilla (control), and RH30-sh$S1PR_1$ cells inoculated into the hind limb muscles of SCID/Beige inbred mice. Five weeks later, mice were sacrificed and femora harvested to evaluate the size of the growing tumor. **$p<0.01$ compared with the control. **Panel E -** Detection of human RMS cells in bone marrow (BM), liver, lung, and peripheral blood (PB) by qRT-PCR. The results are shown as means ± SD. *$p < 0.05$ or **$p < 0.01$.

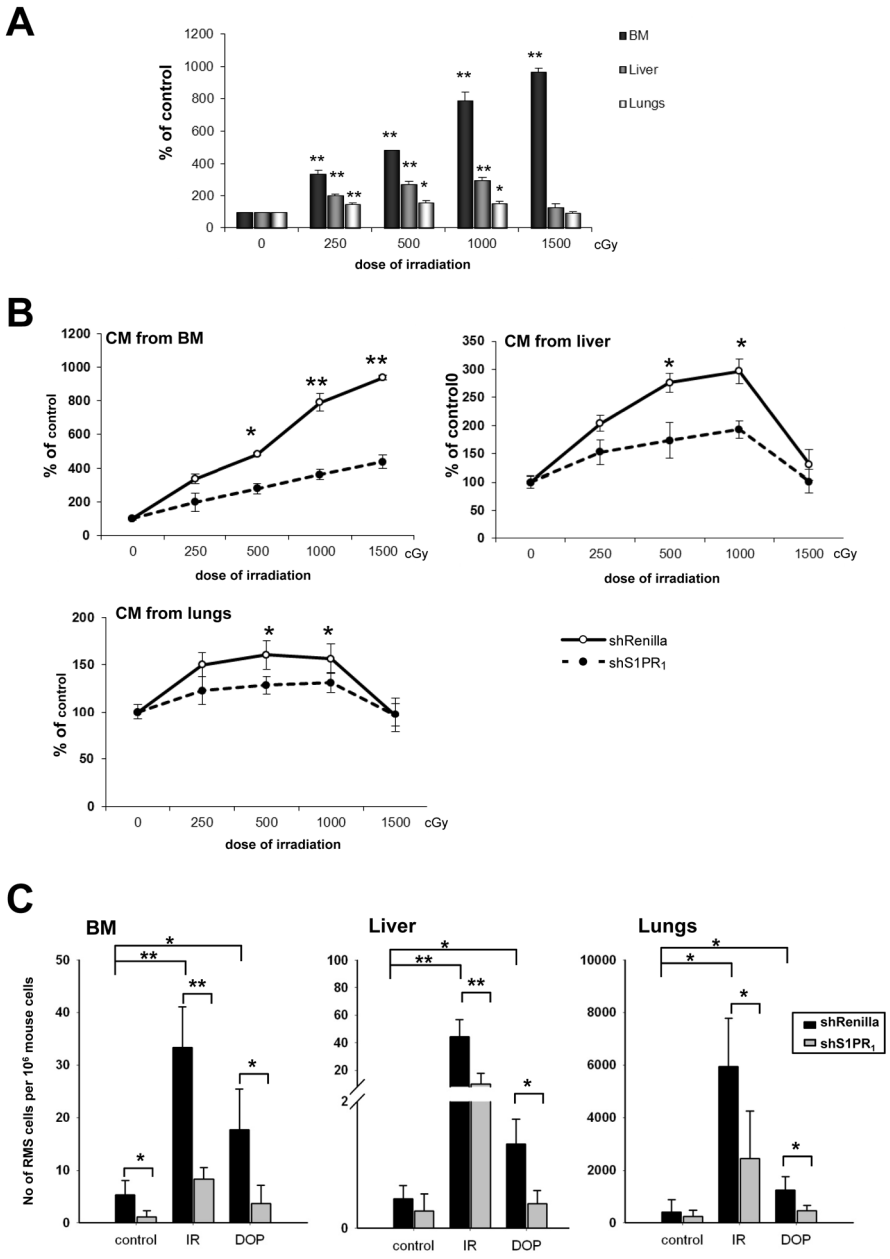

Figure 5. S1P and C1P levels create a pro-metastatic microenvironment in irradiated organs

Panel A – Conditioned media (CM) from irradiated BM, liver, and lung cells enhance migration of RH30 cell lines across Transwell membranes. The results from three independent experiments are shown as means ± SD. *p < 0.05 or **p < 0.01 compared with the control (CM from cells from non-treated animals). **Panel B -** Differences in migration in response to CM between control (shRenilla) and cells with downregulation of S1PR1 (shS1PR1). **Panel C** - Detection of human RMS cells in organs after irradiation or DOP administration. In the experiment, five mice were employed per group. The results are shown as means ± SD. *p < 0.05 or **p < 0.01.

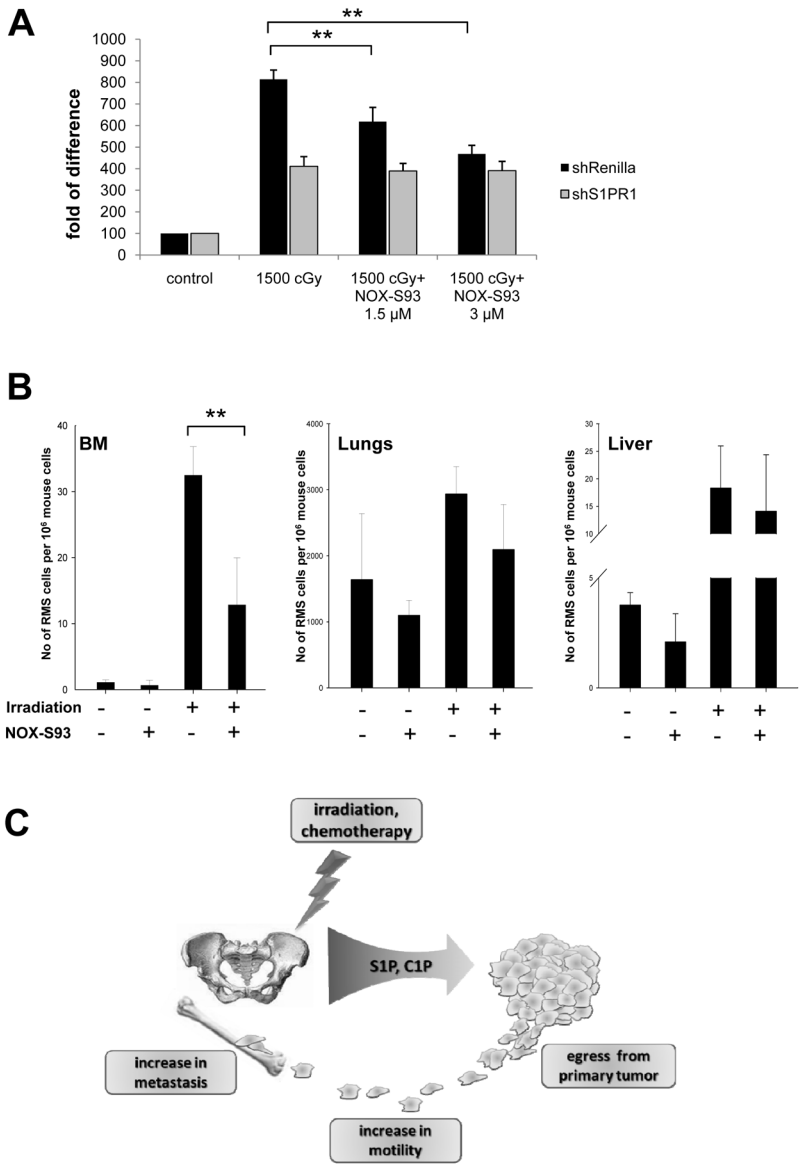

Figure 6. NOX-S93 inhibits S1P-dependent metastasis of RMS to irradiated organs

Panel A – NOX-S93 inhibits dose-dependently the migration of control (shRenilla) RMS cells induced by conditioned medium (CM) from irradiated BM (1500 cGy), whereas it has no effect on RMS cells with knockdown of S1PR1 (shS1PR1). The results from three independent experiments are shown as means ± SD. *$p < 0.05$ or **$p < 0.01$ compared with the control (CM from cells from non-treated animals). **Panel B** - Detection of human RMS cells in organs after irradiation with or without administration of NOX-S93. The results are shown as means ± SD. *$p < 0.05$ or **$p < 0.01$ compared with the control. **Panel C** – Schematic representation of the S1P and C1P effect on RMS metastasis.